Heliyon 9 (2023) e13555

Contents lists available at ScienceDirect

Heliyon

journal homepage: www.cell.com/heliyon

Research article

A methodology for energy dissipation prediction of the bolt group with non-uniform preload

Kepeng Sun, Qingchao Sun *, Binbin Zhao, Yingzhong Zhang, Xuewei Liu

School of Mechanical Engineering, Dalian University of Technology, 116024, Dalian, China

ARTICLE INFO

Keywords:
Bolted joints
Hysteresis behavior
Non-uniform preload
Preload Co-Occurrence matrix
Energy dissipation

ABSTRACT

The bolted joints exhibit typical nonlinear hysteresis under tangential loading, and the deviations of the preload in the bolt group add to the complexity of the model describing this behavior. In this paper, based on the mechanical analysis of the bolt group, a new methodology for predicting hysteresis behavior under non-uniform preload was proposed. Firstly, based on the moment equilibrium within the framework of material mechanics and the tangential stiffness model of the joint interface, a new coordination equation of displacement and force between the bolted joints was deduced, which could realize the calculation of the bolt group loading curve. Then, the PCOM (Preload Co-Occurrence Matrix) was constructed considering the arrangement of the joints, and the indices related to the spatial distribution of the preload were extracted from PCOM. The results of GCA (Grey Correlation Analysis) showed that the indices of PCOM were closely related to the hysteresis behavior of the bolt group. Finally, the prediction of energy dissipation could be realized by using the indices extracted from PCOM and the SVM(Support Vector Machine) regression model. The prediction results were in good agreement with the simulation and experiment, which verified the validity of the methodology proposed in this paper.

1. Introduction

The bolted connection is a widely accepted connection method in the fields of mechanical structure, chemical industry and dynamic engineering. Connected members are brought into contact by bolt preload and transmit tangential loads by dry friction. The bolted connection exhibits nonlinear hysteresis characteristics under the tangential friction [1,2], in which the energy dissipation of the bolted connection accounts for more than 90% of structural energy loss [3–7]. The evolution of the tangential behavior of the bolted connection will directly affect the overall structure's performance. Therefore, the tangential behavior of the bolt group should be considered carefully in predicting dynamic responses.

In recent years, the dynamic responses of bolted joint structures have been extensively studied, especially on the description of the tangential friction behavior at contact surfaces, from stiffness softening [8–12], the nonlinear modeling of tangential stiffness [13–16], and the physical modeling based on the interface topography [17–20]. Considering the inconsistency between the scales related to the energy dissipation and the overall structure, Daniel J. Segalman [21] based on the experimental values in Iwan's framework [22], presented a four-parameter Iwan model to reproduce an experimentally observed power-law relation between the energy dissipation per cycle and the amplitude of applied loads in case of small amplitude oscillatory loads.

* Corresponding author.
E-mail address: qingchao@dlut.edu.cn (Q. Sun).

https://doi.org/10.1016/j.heliyon.2023.e13555
Received 27 November 2022; Received in revised form 6 January 2023; Accepted 3 February 2023
Available online 9 February 2023

In the design of the bolted joint, the connection should have sufficient strength to resist the force produced during the operation. Meanwhile, to prevent the failure of the structure under extreme working conditions, the stable and reliable connection stiffness and energy dissipation capability should be guaranteed through the appropriate design of the system, components and bolted joints, that is, to ensure the flexibility of the bolted connection. Sheng-Jin Chen [23] greatly improved the ductility of the connection structure by optimizing the structure with ultimate strength almost unchanged, while the stiffness decreased slightly. Liu Shuguo [24] used the nonlinear finite element method and experiments to study the dynamic effects of structural parameters and external loads on the rotor joint stiffness and contact state. And the sensitivity analysis of the critical speed and vibration mode was carried out by the finite difference method. The stiffness of the connecting structure turned out to be the most sensitive variable of the external load.

However, in the bolt-up process, even if a high dimensional accuracy of parts is guaranteed after machining, the preload error is inevitable [25,26] due to the deviation of the material parameters, the rough contact at interface, the manipulation error, etc. In a general way, the deviation of bolt group preload is more than 10% or even reach 30%–40%, and it is hard to eliminate. Many works [27,28] on bolt group slip or stiffness mainly study the effect of structural dimensions and joint arrangement (horizontal or longitudinal) on bearing capacity and deformation, but rarely considered the role of preload deviation and joint interaction.

Preload deviation is an inherent characteristic of the threaded connections, and the hysteretic behavior of a bolt group with non-uniform preload may be significantly different from that of a bolt group with uniform preload. So the objective of this work is to investigate the effect of preload deviation on the behavior of bolted joints. Firstly, the theoretical essence of the hysteresis behavior of bolt group with non-uniform preload and resulting performance deviation under tangential force is proposed based on the mechanics of materials, and after the analysis of the joint interaction, the force-displacement coordination equation is obtained combined with the friction mechanical model of joint interface. Then the PCOM (Preload Co-Occurrence Matrix) is established based on the arrangement of joints and features extracted from PCOM turn out to be sensitive to hysteresis behavior of joints by GCA (grey correlation analysis). Finally, the energy dissipation could be predicted combined with these features based on SVM (support vector machine) regression model and the results are in good agreement with simulation and experiment, which indicate the effect of the spatial distribution of preload. The aim of these analyses is to promote a better understanding of the hysteresis behavior of the bolted joints with non-uniform preload and to provide the modeling basis for the dynamic analysis and the response prediction of the complex bolted structure.

2. Mechanical analysis

The studied elementary bolted joint is presented in Fig. 1, as well as boundary conditions. Two plates are assembled using several bolts, and frictional contact conditions between the plates are set up. The research object in this paper is the slip phenomenon of a row of bolts shaped like Fig. 1 - fluctuations of tangential behavior due to deviations in preload when subjected to uniform line load. This abnormal phenomenon could lead to the difference between the performance of the bolted joints and the design requirements, which may result in the component failure such as out-of-tolerance vibration of rotor, the bolt looseness of wind power generation and fatigue failure in building structures. This analysis could provide a helpful guidance for the design of the bolt group with regard to the bearing capacity and tangential behavior under non-uniform preload in engineering. Generally, the deviation of the preload can be directly controlled.

In this model, when the force at a local joint is greater than the maximum friction force (follow Coulomb's friction law), the mobile plate starts to slip due to the transverse load. Then, under the influence of force and moment, the slip area gradually expands from this slipping joint to the whole mobile plate, resulting in globally slip. In this case, he starting point of the bolt group slip and the process of coordinated deformation may be affected by some mechanism.

In order to clarify this mechanism, the following assumptions are made:

1) The interface slip subjects to Coulomb's friction law, $F_f = \mu F_N$, and the bolted joint could be considered to be static when not reach the maximum friction force.
2) The entire connection could be viewed as a beam model perpendicular to the slip direction and $EI = const$;

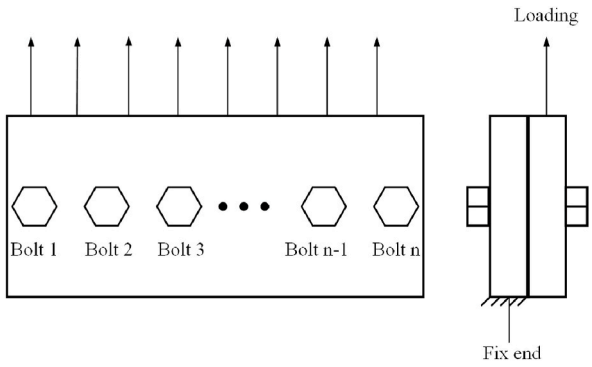

Fig. 1. Description of a row of bolts subjected to the tangential force.

3) The displacement deviation of different joints in the loading direction is very slight, i.e. all joints are almost on the same horizontal line

2.1. Mechanical analysis of bolt group slip

To analyze the tangential constitutive behavior of the bolt group under non-uniform preload, a simple model is established as shown in Fig. 2. To explore the potential mechanism, a row of bolts is simplified as a beam model of material mechanics, and the analysis starts from the occurrence and characteristics of the slip process.

As shown in Fig. 3, the bolted joint without slippage could be regarded as a fixing point and this fixing point divides the connection into two sections, a and b. From the point of view of material mechanics, the size of a, b and the linear load density q will affect the stress and bending moment of the entire connection, thereby affecting the slip process. According to Coulomb's law, the condition for single-bolt globally slip is $q(a+b) > F_{\max f} = \mu F_{pre}$, where $F_{\max f}$ and F_{pre} are the maximum friction and preload respectively. Once meet this condition, the connection would be slippery and unstable, which will affect the performance.

For the two-bolt connection as shown in Fig. 4, the two joints divide the connection into three sections a, b, and c. The slip of the connection is controlled by the load density q and the reaction force of the two joints. In Fig. 4a, when the two joints do not slip, the friction forces in the tensile direction of bolts 1 and 2 do not reach their respective maximum friction forces $F_{\max f1}$ and $F_{\max f2}$. According to the balance of force and moment, the friction force on the two 'fulcrums' can be obtained as: $F_{f1} = \frac{q}{2b}[(a+b)^2 - c^2]$, $F_{f2} = \frac{q}{2b}[(b+c)^2 - a^2]$. The shear force and bending moment of the contact interface continue to increase with the density q, as does the friction force. When the friction force increases to the maximum friction force, the joint slips, as shown in Fig. 4b, and the tangential force at joint 1 is: $F_{\max f1} = \mu F_{pre1}$, where F_{pre1} is the preload of bolt 1. Thus, the tangential force at joint 2 is $F_{f2} = q(a+b+c) - \mu F_{pre1}$. Therefore, for the bolt group, if no slip occurs, the joints will restrict each other under the force and moment balance. For the connection with different dimensions and non-uniform preload, the tangential forces at joints are not the same

If other connection configurations with 3 or more bolted joints are considered, the constraints are more than the degrees of freedom in the slip direction, so that the beam model is transformed into a continuous beam model with more intermediate supports, i.e., a hyperstatic structure. Therefore, the concern has changed from the establishment of the force-moment equilibrium equation to the solution of the physical relationship and the deformation-geometric coordination.

In Fig. 5, there are three fixed fulcrums in the 3-bolt connection when there is no slippage, with the distributed load q and the bending moments M_1, M_3 of sections a and d attached to joint 1 and 3, resulting in the internal bending moment M_2 and support reaction F_{f1}, F_{f2}, F_{f3}. Then the three-moment method (Eq. (1)) [29] was considered to carry out the mechanical analysis of the hyperstatic structure. The three-moment method is mainly suitable for solving the continuous beam problems. For each intermediate support of the continuous beam, a three-moment equation could be listed, and the number of equations listed is equal to the number of intermediate supports of the continuous beam, that is, degree of indeterminacy.

$$M_{n-1}\frac{l_n}{I_n} + 2M_n\left(\frac{l_n}{I_n} + \frac{l_{n+1}}{I_{n+1}}\right) + M_{n+1}\frac{l_{n+1}}{I_{n+1}} = -\frac{6\omega_n a_n}{l_n I_n} - \frac{6\omega_{n+1} b_{n+1}}{l_{n+1} I_{n+1}} \tag{1}$$

Where ω_n and ω_{n+1} are the areas of the bending moment diagram of the simply supported beams of the nth and n+1st spans after the continuous beam is decomposed into simply supported beams. a_n and b_n are the distances between the centroid of ω_n and the left and right supports of the simply supported beam l_n span. I_n is the cross sectional moment of inertia. The beam from joint 1 to joint 2 is assumed to be the first span, and that from joint 2 to joint 3 is assumed to be the second span.

$$M_1 = \frac{qa^2}{2}, M_3 = \frac{qd^2}{2}, l_1 = b, l_2 = c \tag{2}$$

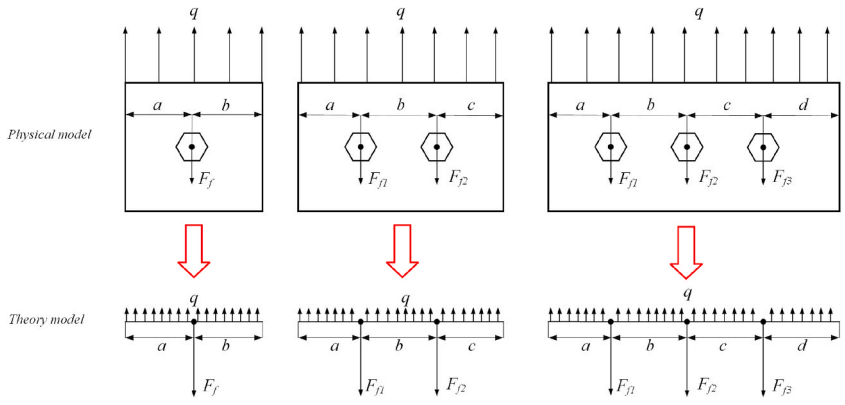

Fig. 2. Theoretical model of the bolt group slip.

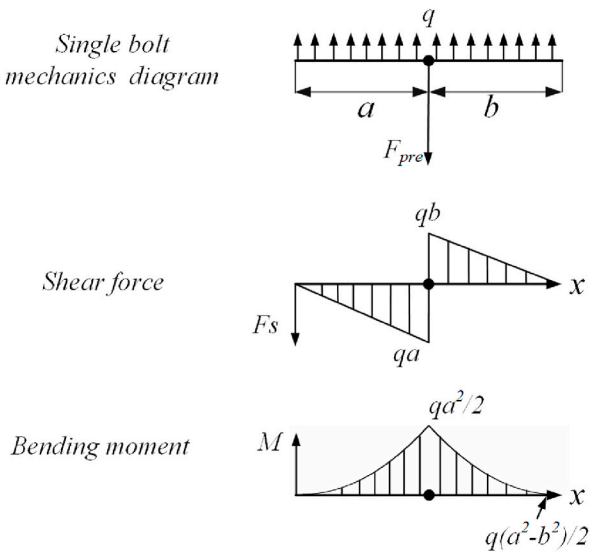

Fig. 3. Shear-bending moment diagram of single-bolt connection.

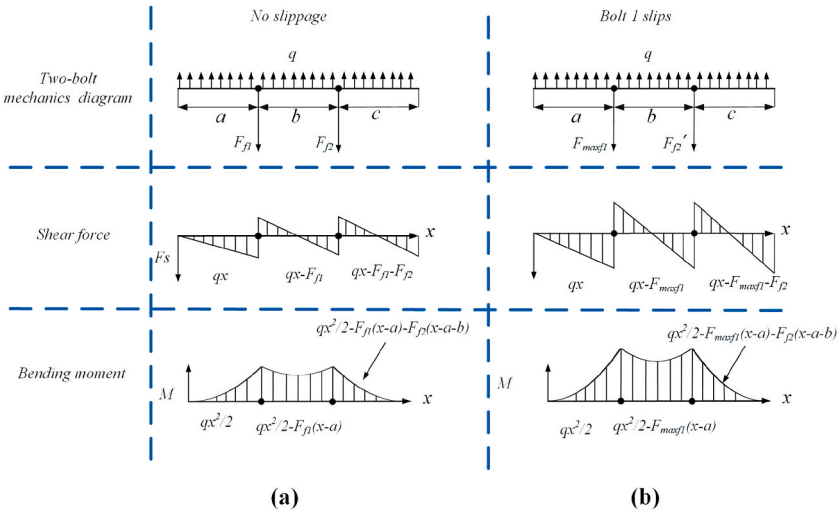

Fig. 4. Shear-bending moment diagram of two-bolt connection. (a) no slippage (b) bolt 1 slips.

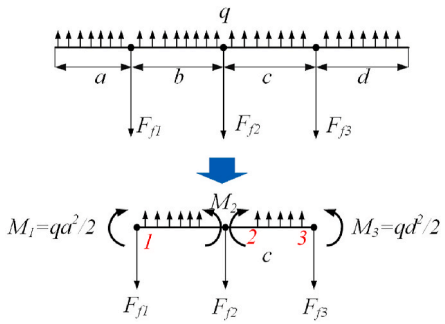

Fig. 5. Mechanical model of the three-bolt connection.

For the section b in Fig. 6, the moment equation is

$$M = \frac{qx^2}{2} - \frac{qb}{2}x = \frac{q}{2}\left(x - \frac{b}{2}\right)^2 - \frac{qb^2}{8} \tag{3}$$

Similarly in section c, $M = \frac{q}{2}\left(x - \frac{c}{2}\right)^2 - \frac{qc^2}{8}$, and each span of the primary statically determinate system is a simply supported beam. Therefore, the bending moment diagram of the two span is shown in Fig. 6 without considering the coordination deformation of the entire continuous beam.

These yield

$$\omega_1 a_1 = \frac{2}{3} \times \frac{qb^2}{8} \times b \times \frac{b}{2} = \frac{qb^4}{24}, \text{similarly}, \omega_2 a_2 = \frac{qc^4}{24} \tag{4}$$

By substitution Eqs. (2) and (4) into Eq. (1)

$$M_1 \times l_1 + 2M_2(l_1 + l_2) + M_3 \times l_2 = \frac{-6 \times \omega_1 a_1}{l_1} - \frac{-6 \times \omega_2 a_2}{l_2} \tag{5}$$

The mechanical equilibrium could be obtained from the primary statically determinate system,

$$\begin{cases} 2M_2(b + c) + cM_3 = \dfrac{qc^3}{4} - \dfrac{qb^3}{4} - \dfrac{qa^2 b}{2} \\ M_3 = \dfrac{qd^2}{2} \end{cases} \tag{6}$$

The support reaction force could be given by Eqs. (1)-6)

$$\begin{cases} F_{f1} = \dfrac{M_1 - M_2}{b} + \dfrac{qb}{2} = \dfrac{q\left(6a^2 b + 4a^2 c - c^3 + b^3 + 2cd^2\right)}{8b(b + c)} + \dfrac{qb}{2} \\ F_{f3} = \dfrac{M_3 - M_2}{c} + \dfrac{qc}{2} = \dfrac{q\left(4bd^2 + 6cd^2 - c^3 + b^3 + 2a^2 b\right)}{8c(b + c)} + \dfrac{qc}{2} \\ F_{f2} = q(a + b + c + d) - F_{f1} - F_{f3} \end{cases} \tag{7}$$

When a certain joint slips, the whole connection degenerates into a two-bolt joint model and the force can be calculated according to the two-bolt model, and then judge the next joint that would slip compared with the maximum friction force. In conclusion, the mechanical analysis of the bolt group with non-uniform preload could be conducted by the statics equilibrium and deformation-force coordination equations. Through the analysis, the support reaction force of the joints at various positions before they do not slip can be obtained. When the support reaction force is greater than the maximum friction force, the bolt joint fails, and the maximum friction force becomes a constant in the opposite direction to the tangential load.

For bolt groups with higher degree of indeterminacy, three-moment method could be also used to calculate the reaction force of each joint under the external tangential load. When the reaction force of some bolts is greater than the maximum friction force, the connection will slip locally. As the external load increases, the degree of indeterminacy of the bolt group model decreases gradually, and then degenerate into a 2-bolt model and a 1-bolt model finally until the entire bolt group slips globally, which affects the performance of the connection.

2.2. Theoretical modeling of tangential stiffness of the bolt group

The stiffness evolves nonlinearly when the bolt joint is subjected to tangential load as shown in Fig. 7. If a certain magnitude of cyclic tangential displacement is applied, the force-displacement curve exhibits obvious hysteretic characteristic. A typical hysteresis curve for the bolted lap plates consists of three parts (Fig. 7): Stage I, stick region; Stage II, nonlinear transition stage with partial slip; Stage III, globally slip region. Therefore, the area enclosed by these three regions was selected as the comprehensive evaluation indice of the tangential hysteresis behavior of the bolt group in this paper, that is, the energy dissipation S_e . The nonlinear evolvement of stiffness at each joint needs to be considered in the multi-bolt model. Referring to Zhao [7], the relationship between the displacement and stiffness of a single bolt joint is given by

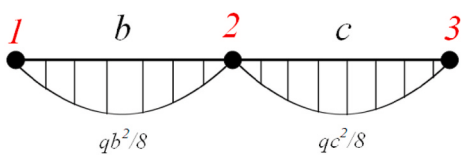

Fig. 6. Two spans of the continuous beam.

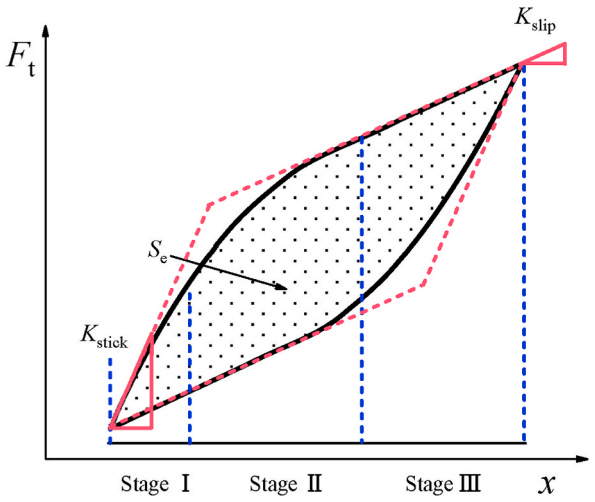

Fig. 7. The hysteresis curve of the bolted joints.

$$K_T(x)=\begin{cases}\dfrac{2(K_{stick}-K_{slip})}{(R_{\max}-R_{\min})\varphi_m}\cdot\left[\dfrac{(R_{\max}-R_{\min})x^2}{2\varphi_m}-R_{\max}x+\dfrac{(R_{\max}-R_{\min})\varphi_m}{2}\right]+K_{slip} & 0\le x\le\varphi_m\\ K_{slip} & x\ge\varphi_m\end{cases} \tag{8}$$

Where K_{stick} and K_{slip} are the tangential stiffness of the joint in the stick region and globally slip region, respectively. $R_{\max}$ and $R_{\min}$ are the maximum and minimum radii of the pressure cone. x is the displacement of the joint and φ_m is the displacement at the transition from stage II to stage III.

The tangential behavior of bolted group is affected by the hysteresis characteristics of bolted joints and the spatial constraints due to structural arrangement and preload. Taking the three-bolt model as an example, the displacement-force coordination equation is obtained by combining the analysis in Section 2.1 and Eqs. (7) and (8).

$$x_1=\frac{F_{f1}}{K_T(x_1)},x_2=\frac{F_{f2}}{K_T(x_2)},x_3=\frac{F_{f3}}{K_T(x_3)} \tag{9}$$

The stiffness of the bolt group is given by

$$K_{group}=K_T(x_1)+K_T(x_2)+K_T(x_3) \tag{10}$$

2.3. FEM simulation

In order to clarify the effect of deviation in the preload on the hysteresis performance of the bolt group straightaway, the simulation of the three-bolt model was performed (Fig. 8). In the simulation model, the fixed constraint was imposed on one end, and the sinusoidal force load with an amplitude of F_t was applied on the other end. The friction coefficient μ of all contact was 0.15 and the loading end generated relative displacement under the sinusoidal force load. The displacement and force charted the hysteresis curve shown in Fig. 8 and the energy dissipation S_e in one loop was extracted from the simulation model.

As shown in Fig. 9, it was assumed that the rated preload of each bolt of a certain connection structure was 10000 N. Due to the

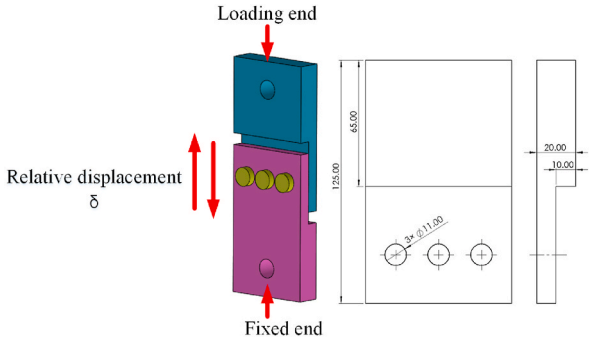

Fig. 8. Simulation of the three-bolt model.

influence of random assembly process parameters (such as torque), the preloads of the three bolts were 8000 N, 10000 N, 12000 N respectively, and the total tangential force of 6750 N was applied. The loading force/displacement curves and contact states of three bolts in the sliding process were extracted from the simulation model. When the bolt pretightening force was imposed but the tangential load is not applied, the bolt connection was in the intact contact state and no local slip occurs.

With the increase of tangential force, when the tangential force reached 4300 N, bolt 1 with 8000 N began to slip locally. It could be clearly seen from Fig. 9a that the distribution of normal and shear stress was not uniform, and the friction stress was generated along the direction perpendicular to the tension, in which some of the bolt preload was decomposed to overcome the tangential stress. When the tangential force reached 4920 N, bolt 2 with 10000 N began to slip, which was earlier than the bolt group with uniform 10000 N preload (5100 N). Because bolt 1 with 7000 N had slipped and cannot bear more tangential force, part of the tangential force was transferred to bolt 2 with 10000 N and bolt 3 with 12000 N. In short, excess torque needs to be borne. At this time, bolt 3 with 12000 N had a small amount of slip, and it could bear greater tangential force. When the tangential force reached 5699 N, slip occurred in bolt 3 with 12000 N, and the whol bolt group cannot bear larger tangential force and slipped macroscopically. (regardless of the bolt rod against the hole).

As shown from the loading curve in Fig. 9b, there was a significant deviation between the model with uniform and non-uniform preload, especially the point where globally slip occurred and the final deformation, which was actually attributed to the joint interaction in Stage I and Stage II mentioned in section 2.2.

What is noteworthy is that the bolt with the lowest preload may not be the first to slip, and the effects of the adjacent bolts torque and other boundary conditions need to be considered (mentioned in the analysis of Section 2.1). Therefore, although the stick and micro-slip stage only account for a small part of the whole slip process, its development determines the final state of the bolt group, which will have a significant impact on the overall performance of the bolt group. All these results from the spatial dispersion of the preload during the initial assembly.

5 preload configurations and 15 arrangements of the three-bolt model were considered, and the results are shown in Figs. 10 and 11. Fig. 10a-d showed the loading curves obtained in the simulation model and the theoretical calculation for three different configurations 9000-10000-11000, 7000-10000-13000, and 8000-10000-12000 respectively, in which the theoretical curves were obtained from Eqs. 7–10. Fig. 11 shows the S_e for all 15 arrangements. In Fig. 10a-d, with the increase of the tangential force, the bolt group gradually transitioned from stage I to stage III. And the higher the dispersion, the lower the stiffness of the bolt group, especially in stage II and stage III; the simulation results were in good agreement with the theoretical calculation.

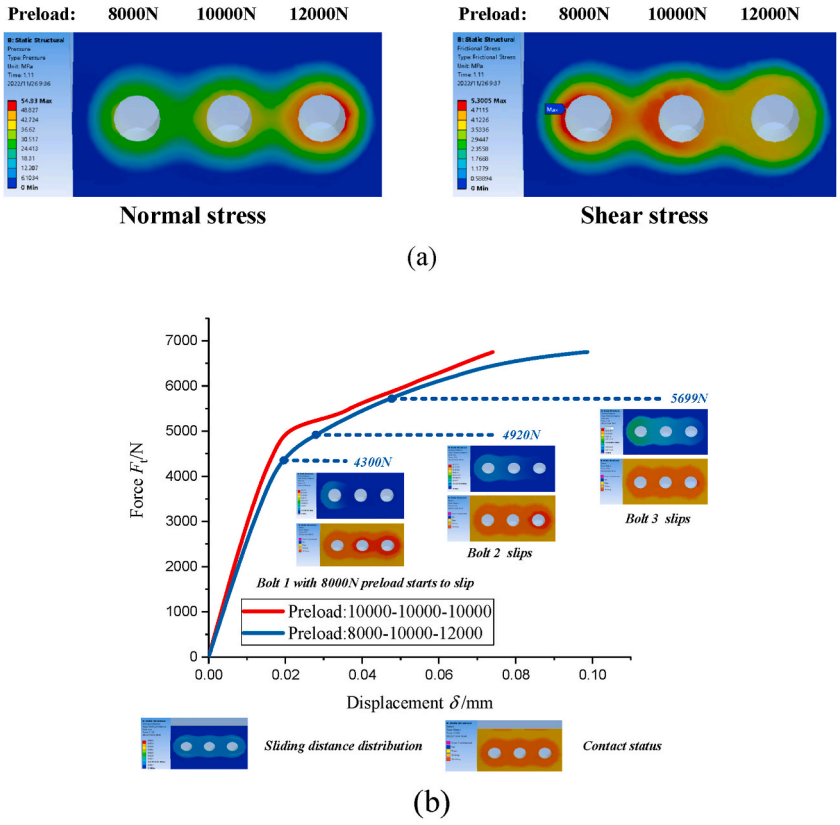

Fig. 9. (a) Normal and tangential stress distribution of contact surface when bolt 1 slips. (b) Comparison of loading curves of models with uniform and non-uniform preloads.

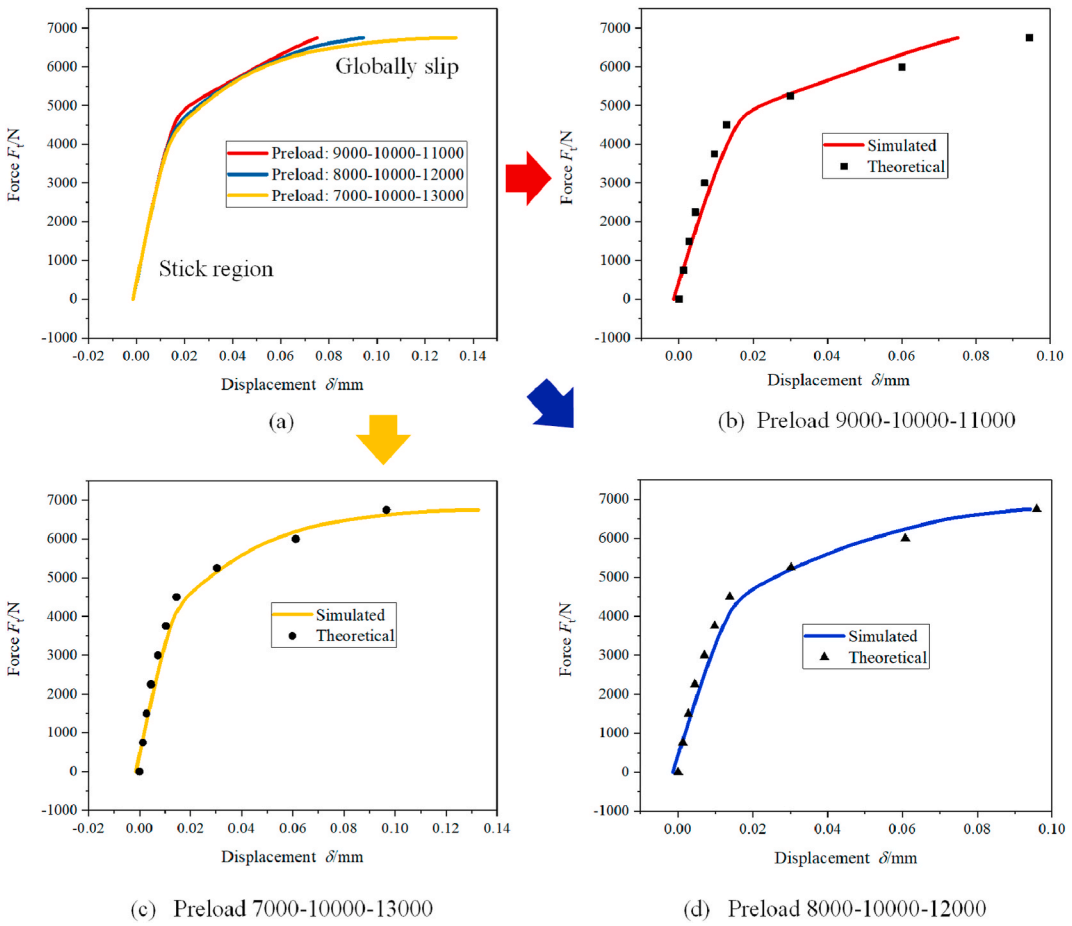

Fig. 10. (a) Loading curves of the three-bolt model with three different preload configurations. (b) comparison of the simulation and theoretical calculation of the preload 9000-10000-11000 N. (c) comparison of the simulation and theoretical calculation of the preload 7000-10000-13000 N. (d) comparison of the simulation and theoretical calculation of the preload 8000-10000-12000 N.

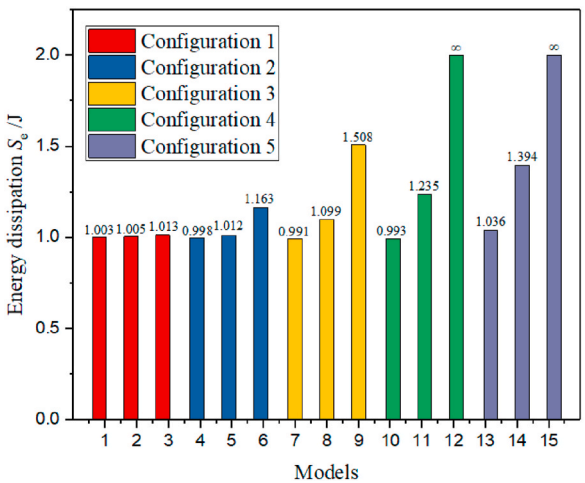

Model	F_{pre1}	F_{pre2}	F_{pre3}	Sum	μ	F_t	$Fv/(\mu \cdot Sum)$	S_e
1	10000	9000	11000	30000	0.15	6750	1.5	1.003
2	9000	11000	10000	30000	0.15	6750	1.5	1.005
3	9000	10000	11000	30000	0.15	6750	1.5	1.013
4	10000	8500	11500	30000	0.15	6750	1.5	0.998
5	8500	11500	10000	30000	0.15	6750	1.5	1.012
6	8500	10000	11500	30000	0.15	6750	1.5	1.163
7	10000	8000	12000	30000	0.15	6750	1.5	0.991
8	8000	12000	10000	30000	0.15	6750	1.5	1.099
9	8000	10000	12000	30000	0.15	6750	1.5	1.508
10	10000	7500	12500	30000	0.15	6750	1.5	0.993
11	7500	12500	10000	30000	0.15	6750	1.5	1.235
12	7500	10000	12500	30000	0.15	6750	1.5	∞
13	10000	7000	13000	30000	0.15	6750	1.5	1.036
14	7000	13000	10000	30000	0.15	6750	1.5	1.394
15	7000	10000	13000	30000	0.15	6750	1.5	∞

Note: ∞ denote that permanent relative slip occurs at the bolted interface, at this point, the bolt connection could be seen as a failure.

Fig. 11. Simulation results of energy dissipation of 15 preload arrangements.

It can be seen from Fig. 11 that the deviation and arrangement of the preload have a great influence on the energy dissipation capacity of the bolt group. Energy dissipation increases with the variance of the preload, implying that bolt group with poor uniformity preloads is more likely to slip, resulting in larger energy dissipation. For bolt groups with the same configuration, i.e. the same variance, different arrangements will lead to differences in energy dissipation. As the variance increases, these differences are magnified, and energy dissipation fluctuates in a wider range, until the failure mode of models 12 and 15 with the permanent slip. The permanent slip means a change in the centroid of the bolt group hysteresis curve. This implys that the position of the preload value in one configuration will also affect the hysteresis behavior of the bolt group.

It is not difficult to imagine that the spatial arrangement of the bolts (for the actual assembly process, the spatial dispersion of the preload) has a significant impact on the performance of the bolt group. In order to achieve accurate prediction of the bolt group performance with large preload dispersion, it is necessary to study the influence of preload spatial dispersion on performance, and the preload dispersion also needs to be expressed spatially.

3. PCOM

From the analysis in Section 2, the bolt group is subject to the hysteresis of the joints during tangential loading, and there are complex interactions and restrictions among the joints due to the structure configuration and the preload value, which further increases the complexity of the performance prediction of the bolted joints. Therefore, the PCOM (Preload Co-Occurrence Matrix) was established based on the concept of co-occurrence matrix [30,31], which was used to model the relationship between the preload and the performance, skipping the coupled effects of complex mechanical analysis and nonlinear hysteresis behavior. The basic idea is to matrix the preload distribution of the bolted joints and extract the features related to the spatial distribution, which are expected to have strong robustness to the hysteresis of the bolt group.

3.1. Construction of PCOM

The preload co-occurrence matrix is essentially a tool used to describe the spatially inhomogeneous characteristics among the interrelated elements within a set, and aims to describe the spatial distribution and interdependence of the preload using the conditional probability distribution of the preload. The construction of PCOM is shown in Fig. 12. A preload-scale distribution in matrix form is first discretized into an integer matrix by dividing the continuous preload value range into n equal width bins, called preload levels, and values in a bin get mapped to a single preload level (Fig. 12a and b). The elements of PCOM are calculated based on this discretized bolt group by counting how often pairs of bolts with specific preload levels and in a specified spatial relationship occur in the matrix (Fig. 12c). The generic element of this matrix is noted $p(i.j)$. The $p(i.j)$ of PCOM can be defined in two different distances: 1-unit and 2-unit length (Fig. 12d). For illustration, 1-unit length (the preload pairs of the adjacent bolts) is selected in Fig. 12c–f. Based on the value of preloads and $p(i.j)$, PCOM indices can be computed (Fig. 12f).

14 PCOM indices have been initially selected, and their meanings and formulas are presented in Table 1. It is worth noting that there are two preload co-occurrence matrices for the bolt group with different spacings (1-unit length and 2-unit length), so in the calculation, contrast of PCOM for 1-unit length is denoted by *Con*1 and *Con*2 for 2-unit length.

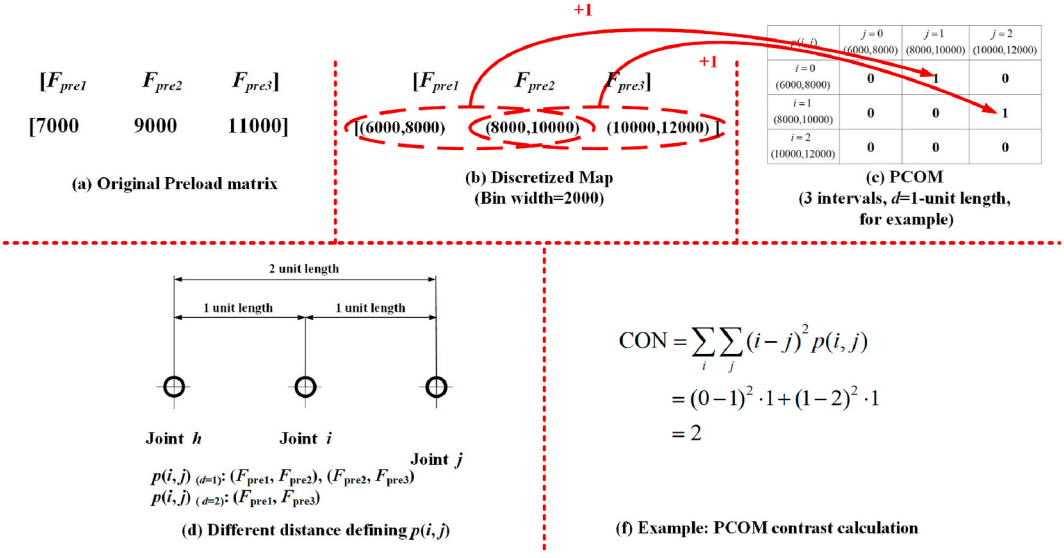

Fig. 12. Illustration of computing PCOM indices for the 3-bolt model.

Table 1
Selected PCOM indices.

Indices	Description	Formula
Contrast: *Con*1, *Con*2	Measeures the drastic change in preload level between bolt joints. High contrast value features large scatter.	$Con = \sum_i \sum_j (i-j)^2 P(i,j)$
Correlation: *Cor*1, *Cor*2	Measeures the linear dependency in the preload matrix. High correlation values imply a linear relationship and more uniform spatial distribution between the preload levels of the adjacent bolt joints.	$Cor = \frac{\sum_i \sum_j (i-\mu)(j-\mu)p(i,j)}{\sigma^2}$
Dissimilarity: *Dis*1 , *Dis*2	Similar to contrast. Instead of weighting the elements exponentially, dissimilarity increases linearly.	$Dis = \sum_i \sum_j \lvert i-j \rvert \cdot P(i,j)$
Homogeneity: *Hom* 1, *Hom* 2	Measeures preload distribution homogeneity, representing the similarity in a preload level between adjacent joints.	$Hom = \sum_i \sum_j \frac{1}{1+(i-j)^2} \cdot P(i,j)$
Mean: $\mu_x 1$, $\mu_x 2$ $\mu_y 1$, $\mu_y 2$	Measeures the average of preload level in the bolt group.	$\mu_x = \sum_i \sum_j i \cdot P(i,j)$ $\mu_y = \sum_i \sum_j j \cdot P(i,j)$
Variance: *Var*1, *Var*2	A measure of heterogeneity, variance increases when the preload values differ from the mean.	$Var = \sum_i \sum_j (i-\mu)^2 P(i,j)$

Note: $p(i,j)$ is the entry (i,j) in the PCOM, μ is the PCOM mean, and σ^2 is the PCOM variance.

3.2. Energy dissipation prediction by SVM

14 PCOM indices can be obtained from Table 1, but the hysteresis behavior is not particularly sensitive to all features. Therefore, based on GCA (grey correlation analysis), all features were scored to select the most sensitive features to hysteresis performance. Finally, the prediction of the hysteresis performance at different preload levels was carried out based on SVM (Support Vector Machine) regression model.

➢ *GCA(Grey Correlation Analysis)*

The GCA can measure the sensitivity of the hysteresis to different features by relevancy degree. Firstly the reference array (research object) and the comparison array (sensitive feature) should be determined when conducting GCA. And then the degree and the order of the relevancy were obtained by mathematical matrix operations. The relevancy coefficient has a certain influence on the relevancy degree calculation. The relevancy coefficient is given by

$$\zeta_i(k) = \frac{[\min_i \min_k |X_i(k) - X_o(k)| + \rho \max_i \max_k |X_i(k) - X_o(k)|]}{[|X_i(k) - X_o(k)| + \rho \max_i \max_k |X_i(k) - X_o(k)|]} \tag{11}$$

When $X_o = \{X_o(k)\ ,\ \ k = 1, 2, \cdots, m\}$ is the reference array and $X_i = \{X_i(k), k = 1, 2, \cdots, m;\ i = 1, 2, \cdots, n\}$ is the comparison array. ρ is the resolution coefficient from 0 to 1, and 0.008 in this work. The relevancy degree can be calculated by

$$\lambda_i = \frac{1}{n} \sum_1^n \zeta_i(k) \quad i = 1, 2, \cdots, n \tag{12}$$

In this paper, the reference array was considered to be highly related to the comparison array when the relevancy degree λ is greater than 0.9.

In order to obtain data on the hysteresis performance of the bolt group under tangential loading, three groups of simulations were carried out, and the 3D model is shown in Fig. 8. The specific settings in simulation are shown in Table 2. The displacement of the loading end was extracted after the simulation and formed the hysteresis curve shown in Fig. 7 combined with the sinusoidal force. Finally, the energy dissipation S_e of each simulation could be obtained.

The S_e obtained by each group of simulations was set as the reference array, and 14 indices ($n = 14$) calculated by the formula in Table 1 were set as the comparison array. The relevancy degree between the indices and S_e of the three groups of simulations is shown in Figs. 13–15 according to Eq. 11 and 12.

From Figs. 13–15, it can be found that most of the indices are highly related to S_e ($\lambda \geq 0.9$), which means that the hysteresis

Table 2
Simulation setting.

Group	F_i/N	Preload distribution interval/N	Sum of preload	Frictional coefficient	Data amount
1	3600	[6000, 12000]	Not limit	0.1	80
2	4000	[6000, 14000]	27000	0.1	50
3	12000	[12000, 36000]	72000	0.1	50

Indices	Relevance
Con1	0.89314
Con2	0.9604
Cor1	0.95773
Cor2	0.98236
Dis1	0.94936
Dis2	0.97786
Hom1	0.92696
Hom2	0.84805
Ux1	0.97697
Ux2	0.97697
Uy1	0.96468
Uy2	0.97697
Var1	0.96812
Var2	0.96812

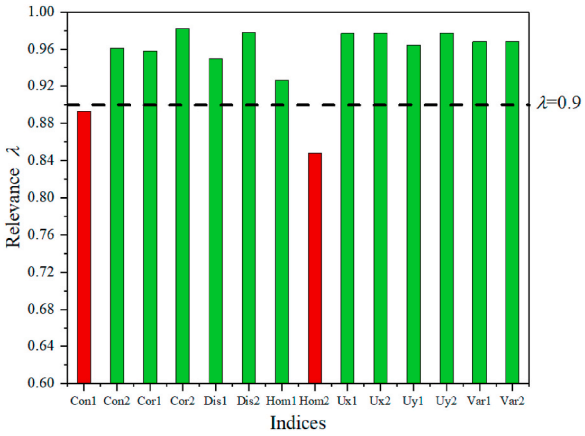

Fig. 13. Relevancy degree calculation of Group 1 simulation.

Indices	Relevance
Con1	0.93071
Con2	0.96351
Cor1	0.9489
Cor2	0.93509
Dis1	0.97118
Dis2	0.9756
Hom1	0.82213
Hom2	0.70735
Ux1	0.98577
Ux2	0.98577
Uy1	0.96992
Uy2	0.98577
Var1	0.98073
Var2	0.98073

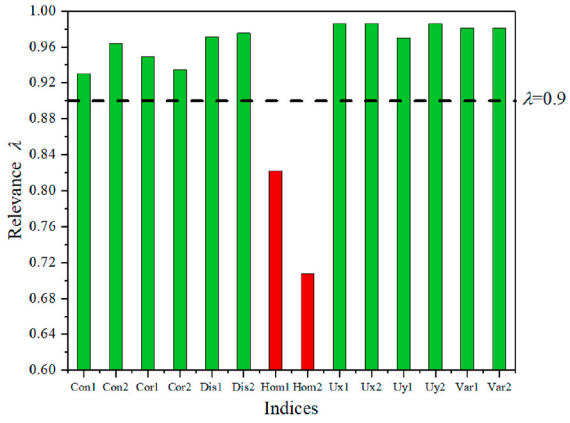

Fig. 14. Relevancy degree calculation of Group 2 simulation.

Indices	Relevance
Con1	0.96087
Con2	0.93899
Cor1	0.97073
Cor2	0.98878
Dis1	0.98221
Dis2	0.97521
Hom1	0.89817
Hom2	0.89144
Ux1	0.99196
Ux2	0.99196
Uy1	0.97895
Uy2	0.99196
Var1	0.98933
Var2	0.98933

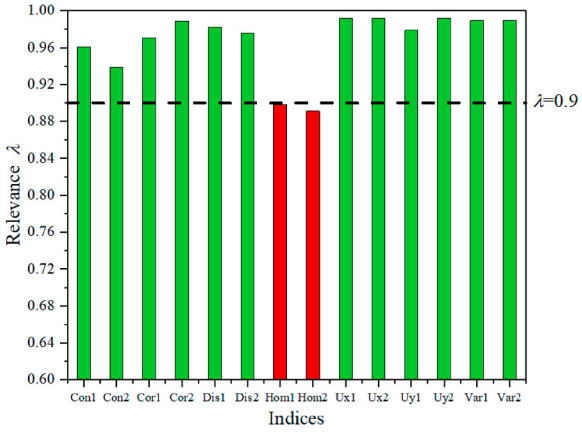

Fig. 15. Relevancy degree calculation of Group 3 simulation.

behavior of the bolt group is closely associated with the spatial distribution of the preload. In general, Mean, Variance and Dissimilarity were the indices with the highest relevancy degree with S_e. These indices focused on the sharp change in preload of neighboring bolts, describing the local aggregation degree of the preload distribution. In practice, the level of Contrast/Dissimilarity increased rapidly when the preload of adjacent bolts changed sharply. The homogeneity measured the similarity of two neighboring preloads, which reflected the clustering of PCOM elements along the diagonal, and therefore yielded a higher value if two neighboring bolts had similar

preloads. However, no matter in which group, *Hom* showed a lower relevancy degree, which meant that the similarity of the preload of the adjacent joints has a less effect on the hysteresis behavior of the bolt group than others. In conclusion, the hysteresis behavior of the bolt group displayed greater sensitivity to the features describing the degree of aggregation component of the preload distribution.

➢ *Energy dissipation prediction by SVM*

Once the assembly process is completed, the PCOM will be generated, and the parameters extracted from PCOM will affect the mechanical response of the bolt group during loading. Inspired by this idea, the SVM (support vector machine) regression model was adopted to capture this nonlinear connection and predict S_e of the bolt group. After GCA was performed on the 14 features in Table 1 and the simulation results, the features with $\lambda \leq 0.9$ were removed. The SVM regression model (five-fold cross validation, the linear kernel function) was used to predict the S_e of the bolt group combined with the simulation data. The results were shown in Fig. 16, in which a-c were the regression prediction results of the Group 1–3 of the simulation models respectively. As can be seen from Fig. 16, the connection between the simulation results and the indices extracted from PCOM could be easily established by the SVM algorithm, and the average error was about 1%. All these analysis had proved that the level and the spatial distribution of the preload were directly related to the performance of the bolt group.

4. Experimental validation

4.1. Experimental setup

In order to verify the validity of the proposed method of hysteresis performance prediction for the multi-bolt model with non-uniform preload, the fatigue tester (Fig. 17) was used to measure the force-displacement curve of the bolt group. The intelligent bolt preload testing system [32] developed by our research team is adopted to calibrate and measure the bolt preload, so as to realize the precise control of the bolt preload during the experiment.

4.2. Experimental results

The indices of PCOM in the experiment were extracted by the program written according to the construction principle of the PCOM and then the method mentioned in section 3.2 was applied to predict the energy dissipation of the corresponding hysteresis curve. The prediction results are shown in Fig. 18 and some experimental test results are shown in Table 3.

As shown in Fig. 18, it is found that there is a good correlation between the experimental results and the prediction, and the prediction error of most samples is within 10%. The reasons for the dispersion of the prediction error is speculated to be as follows: (1) the error of the intelligent bolt preload testing system, which has been calibrated by the force sensor and the error of the preload test is about 3%; (2) machining error of the sample and the bolts, the deviation of the dimension would cause the coefficient conversion error in the calculation of the preload test system, which lead to a certain degree error of preload measurement; (3) Force-displacement measurement error, the measurement error of the fatigue tester will also cause inaccurate results; (4) Friction coefficient dispersion, because of the same lap joint used in the experiment, there existed a limited friction coefficient error.

In conclusion, the method based on the PCOM proposed in this paper successfully captured the dynamic hysteresis behavior characteristics of the bolt group with non-uniform preload, and successfully predicted the energy dissipation. These demonstrate the potential of using the PCOM to characterize the hysteresis characteristics of the bolt group and the applicability of the methodology used in other fields.

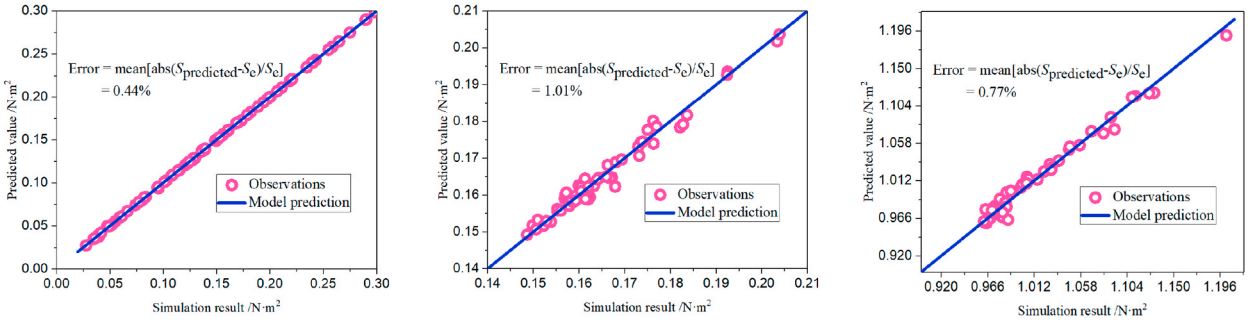

Fig. 16. Prediction results of energy dissipation of (a) group 1, (b) group 2 and (c) group 3 based on SVM algorithm and PCOM indices in FEM analysis.

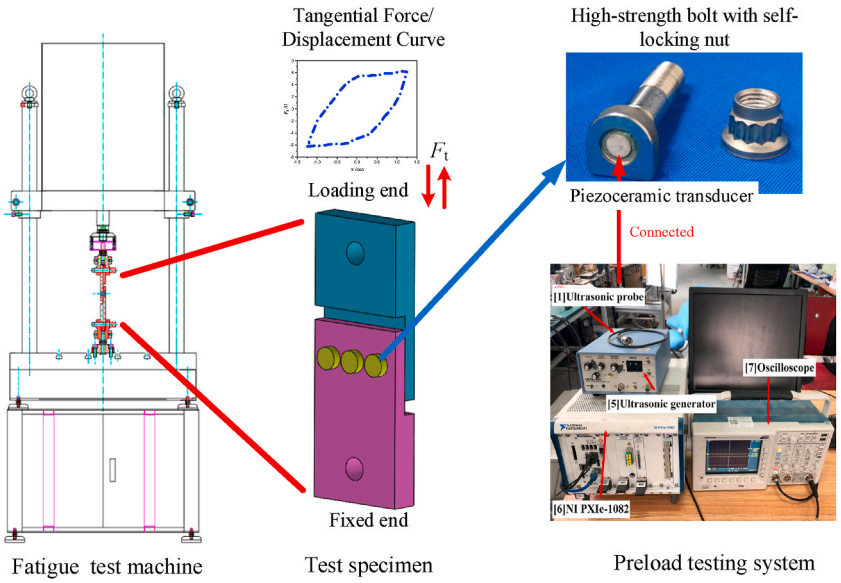

Fig. 17. Specimen clamping and the preload testing system.

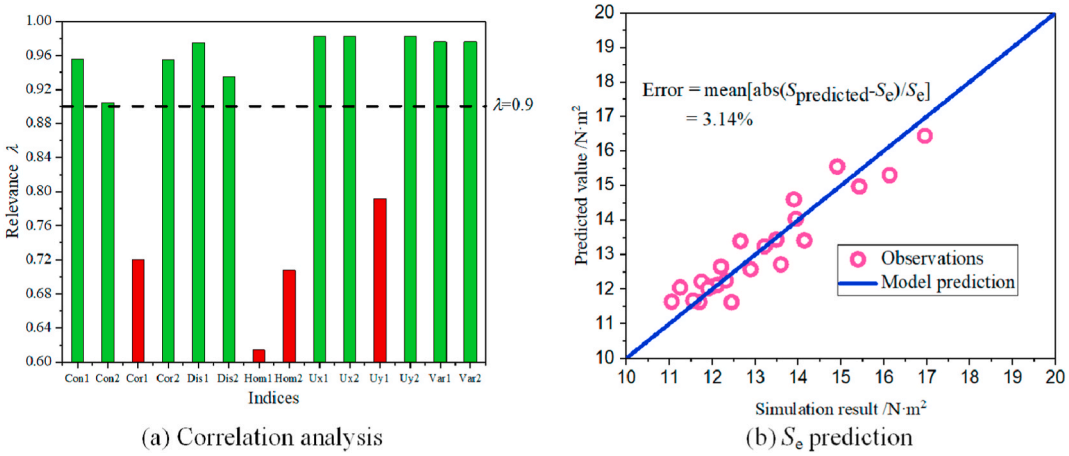

Fig. 18. Feature selection and prediction. (a) GCA analysis in the experiment. (b) Energy dissipation prediction of the experiment.

Table 3
Some of experimental results and prediction.

Num.	F_{pre1}/N	F_{pre2}/N	F_{pre3}/N	F_t/N	*Sum*/N	S_e/J	Prediction/J	Error (%)
1	5729	2686	3920	6000	12335	16.957	16.437	−3.07
2	5491	2656	3711	6000	11858	16.136	15.298	−5.19
3	4539	2809	4397	6000	11745	15.428	14.971	−2.96
4	2737	5011	3831	6000	11579	13.949	14.031	0.59
5	4097	4032	3592	6000	11721	11.901	12.020	0.99

5. Conclusions

This paper presents a new methodology for predicting the hysteresis characteristics of the bolt group with non-uniform preload. Through the mechanical analysis and the simulation verification, it was found that the spatial distribution of the preload had an important influence on the hysteresis performance of the bolt group. In general, the bolt group with poorer preload uniformity tend to have lower tangential stiffness and larger displacements, resulting in greater energy dissipation. In order to skip the complex mechanical analysis and simplify the prediction process of the bolt group performance, the PCOM considering the spatial distribution of

the preload was constructed. The features extracted from PCOM were proved by GCA to be closely related to the hysteresis behavior. Finally, the SVM regression model was adopted to predict the energy dissipation successfully. This methodology was confirmed by the simulation and the experiment.

Declarations

Author contribution statement

Kepeng Sun: Conceived and designed the experiments; Performed the experiments; Analyzed and interpreted the data; Wrote the paper.

Qingchao Sun: - Conceived and designed the experiments; Contributed materials, analysis tools or data.

Binbin Zhao: Performed the experiments.

Yingzhong Zhang: Contributed materials, analysis tools or data

Xuewei Liu: Performed the experiments.

Funding statement

Prof Qingchao Sun was supported by National Natural Science Foundation of China [51875081 & 51935003].

Data availability statement

Data included in article/supp. material/referenced in article.

Declaration of interest's statement

The authors declare no competing interests.

References

[1] D.J. Segalman, M.J. Starr, Relationships Among Certain Joint Constitutive Models (Tech.Rep. SAND2004-4321, Sandia National Laboratories, 2004.
[2] V. Piluso, G. Rizzano, Experimental analysis and modelling of bolted T-stubs under cyclic loads, J. Constr. Steel Res. 64 (6) (2008) 655–669.
[3] E. Brunesi, R. Nascimbene, G.A. Rassati, Response of partially-restrained bolted beam-to-column connections under cyclic loads, J. Constr. Steel Res. 97 (2014) 24–38.
[4] A.B. Sabbagh, M. Petkovski, K. Pilakoutas, et al., Cyclic behaviour of bolted cold-formed steel moment connections: FE modelling including slip, J. Constr. Steel Res. 80 (2013) 100–108.
[5] N. Jamia, H. Jalali, J. Taghipour, et al., An equivalent model of a nonlinear bolted flange joint, Mech. Syst. Signal Process. 153 (2021), 107507.
[6] D. Li, C. Xu, D. Botto, et al., A fretting test apparatus for measuring friction hysteresis of bolted joints, Tribol. Int. 151 (2020), 106431.
[7] B. Zhao, F. Wu, K. Sun, et al., Study on tangential stiffness nonlinear softening of bolted joint in friction-sliding process, Tribol. Int. 156 (2021), 106856.
[8] S.M. Sah, J.J. Thomsen, M. Brøns, et al., Estimating bolt tightness using transverse natural frequencies, J. Sound Vib. 431 (2018) 137–149.
[9] J.J. Meyer, D.E. Adams, Using impact modulation to quantify nonlinearities associated with bolt loosening with applications to satellite structures, Mech. Syst. Signal Process. 116 (2019) 787–795.
[10] R. Verwaerde, G. Pierre-Alain, B. Pierre-Alain, A nonlinear finite element connector for the simulation of bolted assemblies, Comput. Mech. 65 (6) (2020) 1531–1548.
[11] J. Armand, L. Salles, C.W. Schwingshackl, et al., On the effects of roughness on the nonlinear dynamics of a bolted joint: a multiscale analysis, Eur. J. Mech. Solid. 70 (2018) 44–57.
[12] N.N. Balaji, W. Chen, M.R.W. Brake, Traction-based multi-scale nonlinear dynamic modeling of bolted joints: formulation, application, and trends in micro-scale interface evolution, Mech. Syst. Signal Process. 139 (2020), 106615.
[13] R. Lacayo, L. Pesaresi, J. Groß, et al., Nonlinear modeling of structures with bolted joints: a comparison of two approaches based on a time-domain and frequency-domain solver, Mech. Syst. Signal Process. 114 (2019) 413–438.
[14] D. Li, C. Xu, J. Kang, et al., Modeling tangential friction based on contact pressure distribution for predicting dynamic responses of bolted joint structures, Nonlinear Dynam. 101 (1) (2020) 255–269.
[15] C. Li, R. Qiao, Q. Tang, et al., Investigation on the vibration and interface state of a thin-walled cylindrical shell with bolted joints considering its bilinear stiffness, Appl. Acoust. 172 (2021), 107580.
[16] L. Tan, C. Wang, Y. Liu, et al., Study on hysteresis and threaded fitting behavior of bolted joint with non-parallel bearing surface[J], Mech. Syst. Signal Process. 168 (2022), 108655.
[17] M. Eriten, C.H. Lee, A.A. Polycarpou, Measurements of tangential stiffness and damping of mechanical joints: direct versus indirect contact resonance methods, Tribol. Int. 50 (2012) 35–44.
[18] M. Eriten, A.A. Polycarpou, L.A. Bergman, Physics-based modeling for fretting behavior of nominally flat rough surfaces, Int. J. Solid Struct. 48 (10) (2011) 1436–1450.
[19] W. Zhan, P. Huang, Physics-based modeling for lap-type joints based on the Iwan model, J. Tribol. 140 (5) (2018).
[20] L. Li, J. Wang, X. Pei, et al., A modified elastic contact stiffness model considering the deformation of bulk substrate, J. Mech. Sci. Technol. 34 (2) (2020) 777–790.
[21] D.J. Segalman, A Four-Parameter Iwan Model for Lap-type Joints, 2005.
[22] W.D. Iwan, On a class of models for the yielding behavior of continuous and composite systems, ASME J. Appl. Mech. 34 (1967) 612–617.
[23] S.J. Chen, C.H. Yeh, J.M. Chu, Ductile steel beam-to-column connections for seismic resistance, J. Struct. Eng. 122 (11) (1996) 1292–1299.
[24] L. Shuguo, M. Yanhong, Z. Dayi, et al., Studies on dynamic characteristics of the joint in the aero-engine rotor system, Mech. Syst. Signal Process. 29 (2012) 120–136.
[25] Y. Li, Z. Liu, Y. Wang, et al., Experimental study on behavior of time-related preload relaxation for bolted joints subjected to vibration in different directions, Tribol. Int. 142 (2020), 106005.
[26] W.A. Grabon, M. Osetek, T.G. Mathia, Friction of threaded fasteners, Tribol. Int. 118 (2018) 408–420.

[27] Y. Huang, R. Wang, J. Zou, et al., Finite element analysis and experimental study on high strength bolted friction grip connections in steel bridges, J. Constr. Steel Res. 66 (6) (2010) 803–815.
[28] H. Guo, F. Xiao, Y. Liu, et al., Experimental and numerical study on the mechanical behavior of Q460D high-strength steel bolted connections, J. Constr. Steel Res. 151 (2018) 108–121.
[29] L. Hongwen, Mechanics of Materials, Higher education press, Beijing, 2017 (in Chinese).
[30] R.M. Haralick, K. Shanmugam, I.H. Dinstein, Textural features for image classification, IEEE Transact. Sys. Man Cybern, (6) (1973) 610–621.
[31] R.M. Haralick, Statistical and structural approaches to texture, Proc. IEEE 67 (5) (1979) 786–804.
[32] Q. Sun, B. Yuan, X. Mu, et al., Bolt preload measurement based on the acoustoelastic effect using smart piezoelectric bolt, Smart Mater. Struct. 28 (5) (2019), 055005.